ARMY RESEARCH LABORATORY

Processing and Evaluation of 3D-Reinforced Needled Composite Laminate

by Ryan P. Emerson, Jason Cain, Michael Simeoni, and Bradley Lawrence

ARL-TR-6107 **September 2012**

NOTICES

Disclaimers

The findings in this report are not to be construed as an official Department of the Army position unless so designated by other authorized documents.

Citation of manufacturer's or trade names does not constitute an official endorsement or approval of the use thereof.

Destroy this report when it is no longer needed. Do not return it to the originator.

Army Research Laboratory
Aberdeen Proving Ground, MD 21005

ARL-TR-6107 **September 2012**

Processing and Evaluation of 3D-Reinforced Needled Composite Laminate

Ryan P. Emerson
Weapons and Materials Research Directorate, ARL

Jason Cain
Dynamic Sciences, Inc.

Michael Simeoni
Drexel University (Cooperative Education Student)

Bradley Lawrence
Bowhead Science and Technology

REPORT DOCUMENTATION PAGE

Form Approved
OMB No. 0704-0188

1. REPORT DATE *(DD-MM-YYYY)*	2. REPORT TYPE	3. DATES COVERED (From - To)
September 2012	Technical Report	June 2012

4. TITLE AND SUBTITLE
Processing and Evaluation of 3D-Reinforced Needled Composite Laminate

5a. CONTRACT NUMBER

5b. GRANT NUMBER

5c. PROGRAM ELEMENT NUMBER

6. AUTHOR(S)
Ryan P. Emerson[1], Jason Cain[2], Michael Simeoni[3], and Bradley Lawrence[4]

5d. PROJECT NUMBER

5e. TASK NUMBER

5f. WORK UNIT NUMBER

7. PERFORMING ORGANIZATION NAME(S) AND ADDRESS(ES)
U.S. Army Research Laboratory
ATTN: RDRL-WMM-A
Aberdeen Proving Ground, MD 21005

8. PERFORMING ORGANIZATION REPORT NUMBER
ARL-TR-6107

9. SPONSORING/MONITORING AGENCY NAME(S) AND ADDRESS(ES)

10. SPONSOR/MONITOR'S ACRONYM(S)

11. SPONSOR/MONITOR'S REPORT NUMBER(S)

12. DISTRIBUTION/AVAILABILITY STATEMENT
Approved for public release; distribution unlimited.

13. SUPPLEMENTARY NOTES
[1]U.S. Army Research Laboratory, WMRD, Materials Division
[2]Dynamic Sciences, Inc.
[3]Drexel University (Cooperative Education Student)
[4]Bowhead Science and Technology

14. ABSTRACT
This report documents the fabrication and test of a woven glass/epoxy composite laminate that was reinforced in the through-thickness direction with aramid fibers using a needling process. The purpose of reinforcing laminated material in the through-thickness direction is to improve its delamination resistance/damage tolerance. The needled material was approximately 6.4-mm thick and was tested using American Standard Test Method ASTM standards to assess the improvements in impact response and any reductions in-plane strength, which is a typical tradeoff with 3D-reinforced stitched materials. Needled specimens exhibited 10–15% increase in effective stiffness (force-deflection response) under impact loading, and a 50% increase in compression-after-impact strength–a significant improvement in damage tolerance. Needled but non-impacted material exhibited a 9% increase in the in-plane compressive strength and a 17% increase in flexural strength, indicating at least that the needling process does not cause immediate tradeoffs in the in-plane strength of woven glass materials. Because the processing parameters were arbitrarily chosen, these experiments should be considered as proof-of-concept.

15. SUBJECT TERMS
3D, composite, laminate, needling, delamination, damage tolerance, impact

16. SECURITY CLASSIFICATION OF:			17. LIMITATION OF ABSTRACT	18. NUMBER OF PAGES	19a. NAME OF RESPONSIBLE PERSON
a. REPORT	b. ABSTRACT	c. THIS PAGE	UU	26	Ryan P. Emerson
Unclassified	Unclassified	Unclassified			19b. TELEPHONE NUMBER (*Include area code*) (410) 306-0990

Contents

List of Figures

List of Tables

Acknowledgments

The authors wish to acknowledge Mr. Robert Miller for fabricating the semi-automated tooling shown in figure 8.

INTENTIONALLY LEFT BLANK.

1. Introduction

Several approaches have been pursued and documented in the literature for the purpose of improving the delamination resistance of laminated composite materials for ballistic and structural applications. The best current approaches employ one or more varieties of "3D" or through-thickness reinforcement (TTR) including pinned, stitched, tufted, knitted and woven architectures. The myriad combinations of materials, applications/geometry and load spectra preclude conclusive statements on which is the best TTR technology (*1*) but typically the benefits of 3D composites also carry tradeoffs in manufacturability, degradation of in-plane strength, and/or cost.

Tufting is a relatively new process described in the literature for improving the delamination resistance of composite laminates. The tufting process uses a hollow needle to insert glass or carbon threads comprised of typically 1000 to 2000 filaments (*2–5*) through a dry laminate preform. Tufts are typically spaced such that the resultant TTR fiber volume fraction is in the range of 3–5%. Tufting is similar to stitching except that when the needle is retracted the loops are not locked-in with a bobbin thread or chain thread. The architecture resulting from the tufting process is shown schematically in figure 1.

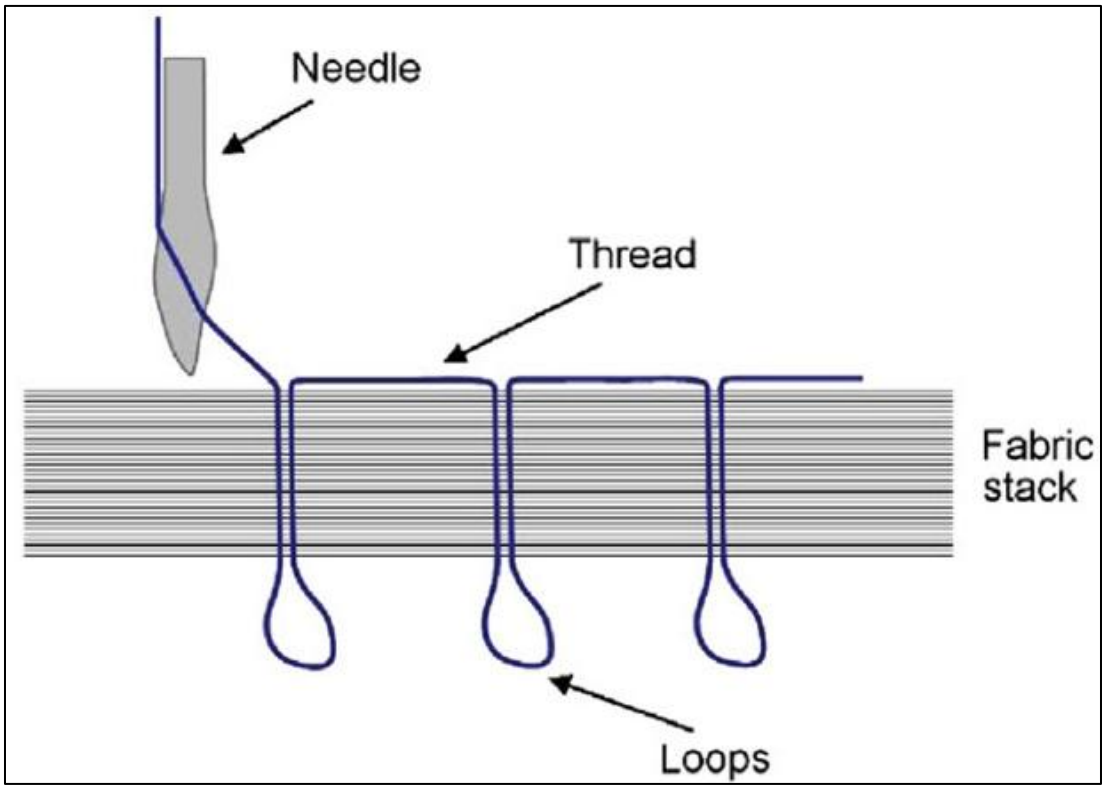

Figure 1. Side-view illustration of a fiber architecture achieved by tufting (*3*).

Another method for achieving a 3D fiber architecture is so-called needling (needlepunching) or felting. Several examples are found in the literature of needled/felted carbon-carbon (C/C) composites for high temperature applications such as ablative aerospace heat shields (*6*) and automobile brake pads (*7*). The needled TTR in these previous reports was created by plunging downward-barbed needles through dry laminates of carbon fiber prior to pyrolisis, essentially breaking some of the in-plane carbon fiber to orient a fraction of the filaments in the through-thickness direction. The flexural strengths of the resultant needled C/C materials were reported in the range of 100–130 MPa and, as such, these materials are not relevant for high strength applications. Non-structural needled aramid fabric laminates are commercially available as air filtration media and in personnel protection products[1].

The literature provides no examples of the needling process and material as described in the present report, wherein needling used to improve the ballistic response of a high-strength structural laminate. Figure 2 is an illustration showing the fundamental components and process of the present application of needling. In this process, the downward-barbed needle picks-up and inserts so-called "supply" material into the 2D laminate.

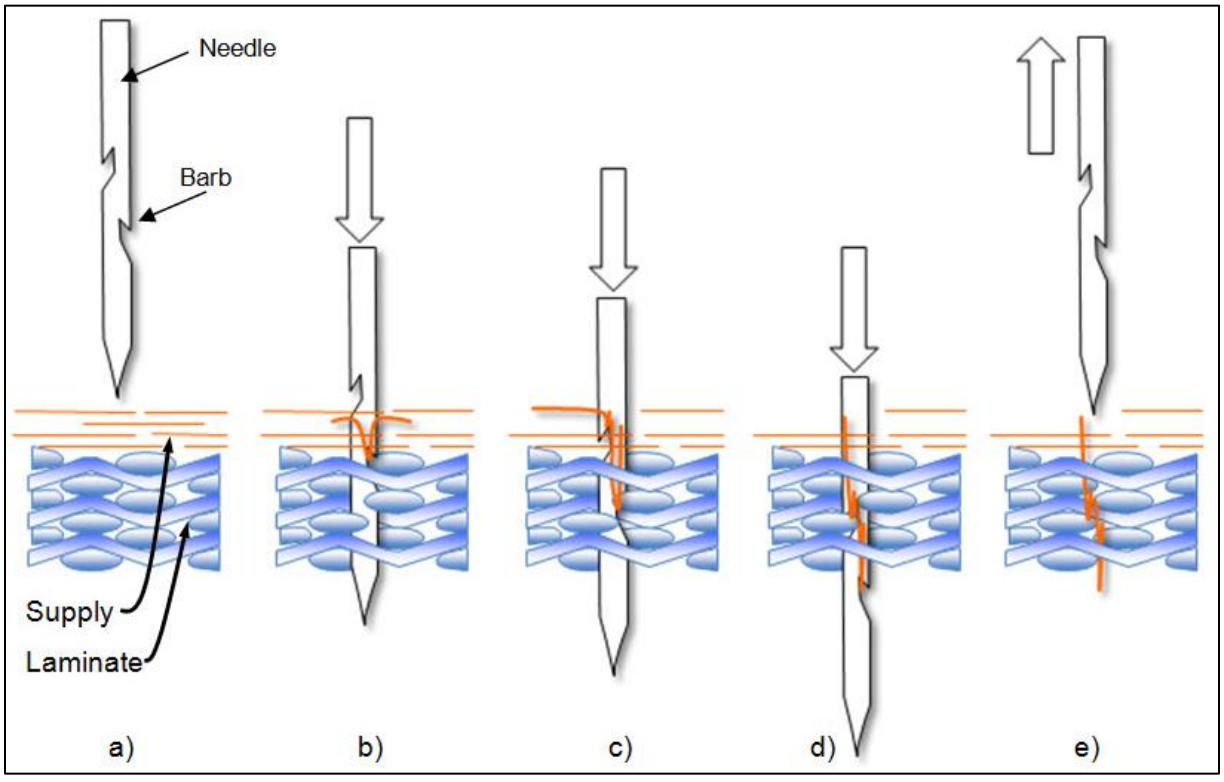

Figure 2. Illustration showing how the needle pushes supply material into the carrier material.

[1] TexTech Industries, Portland, ME.

The most important difference distinguishing needling from tufting or stitching is that needling typically inserts 20–60 through-thickness filaments at each penetration site, whereas the threads used in tufting and stitching are several thousands of filaments. This is significant because in-plane fiber distortion caused by the tuft/stitch thread is identified in the literature as the primary cause for the typical reported 5–15% reduction in the in-plane stiffness and strength (*3*, *4*). Needled TTR should thus incur less reduction in the in-plane strength because the fiber distortions are significantly reduced.

The proof-of-concept needling experiments described in this report were conducted at the U.S. Army Research Laboratory, Aberdeen Proving Ground, MD as part of mission-funded research in durable composite materials. These experiments employed handheld processing methods and off-the-shelf needles designed for clothing and paper textiles (i.e., not optimized for fiberglass, aramid, and carbon). As such, the resulting microstructures are non-optimal and exemplify the current gaps in the understanding of the process variables.

2. Objective/Approach

Considering that process models are unavailable for needled composites, the primary objective of fabricating the specimens described in this report was to gain hands-on familiarity with the needling hardware and materials. Such hands-on exploration was intended to guide the eventual development of a needling process model, specifically a model relating microstructure to the processing parameters. A secondary objective was to assess the impact response and in-plane mechanical strength of needled material.

The approach was to assemble dry "parent" laminates, needle half of the parent laminate (using the other half as control material), and then infuse the laminates using the Vacuum Assisted Resin Transfer Molding (VARTM) process. Specimens were then cut from the cured parent panels and inspected with microscopy and tested using American Standard Test Method (ASTM) standards.

3. Experimental

3.1 Materials/Panels

Figures 3 and 4 show illustrations of the two parent panels fabricated in the present research. The in-plane reinforcement in both panels was eight plies of S2-glass plain weave in a quasi-isotropic layup, $[(45/0)_2]_S$.[2] This material and layup was chosen because it has been used and characterized extensively at ARL. The TTR "supply" for both panels was several plies of random-oriented aramid mat with areal density of 34 g/m^2 per ply.[3] The length of the aramid fibers is approximately 13 mm, and the mat was custom made with a minimum amount of poly-vinyl alcohol binder (just enough for handling purposes). Panel 1 incorporated three plies of the mat needled through the top of the panel and Panel 2 incorporated two plies on top, needled from the top, plus two plies on the bottom, needled from the bottom.

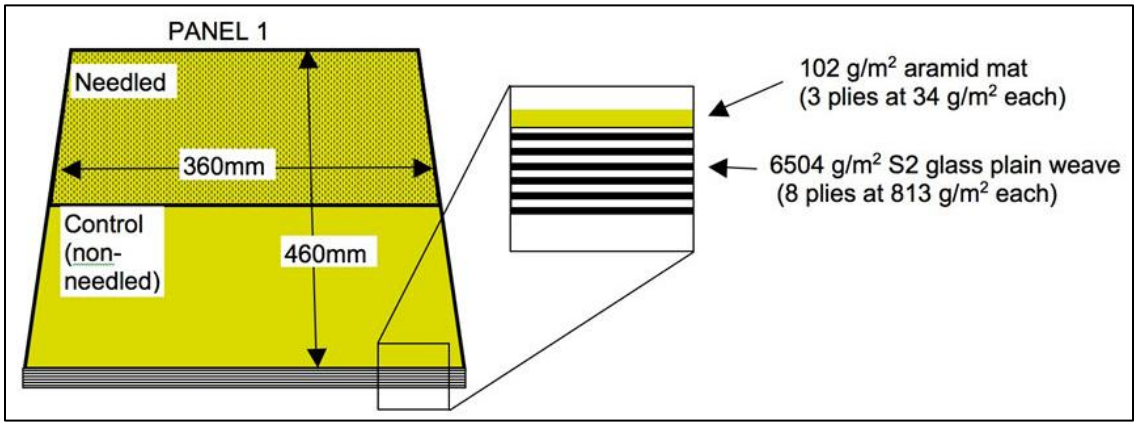

Figure 3. Illustration of Panel 1.

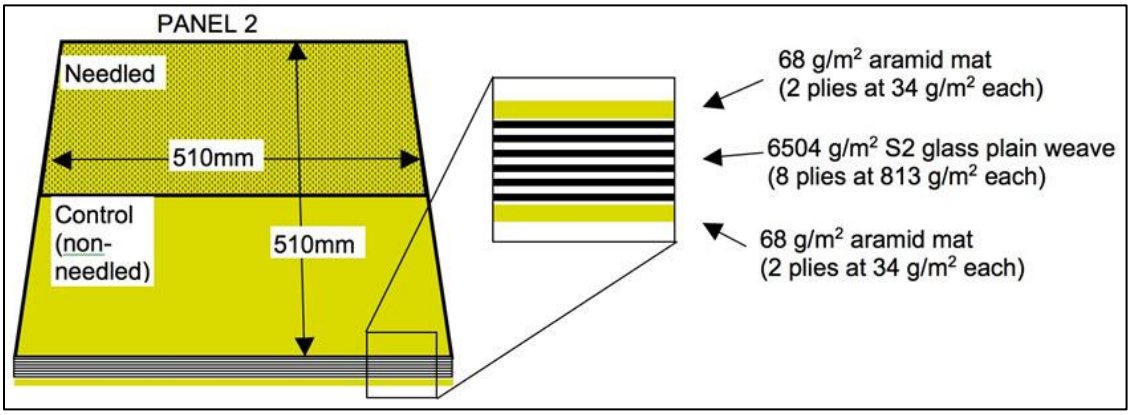

Figure 4. Illustration of Panel 2.

[2] BGF Industries, Greensboro, NC

[3] Technical Fibre Products Inc., Schenectady, NY

3.2 The Needle

The needle used in this investigation is a Colonial brand 36-gage "blue point" with a triangular blade and nine barbs. Figure 5 shows a dimensioned illustration of the needle and barbs (barb numbers 2, 5, and 8 are hidden from this viewpoint). Figure 6 provides more detail on the shape of the barb in this particular needle, showing that the barb actually protrudes beyond the profile of the blade. As such this needle is considered "aggressive" and pushes more supply per punch than other needles (with non-protruding barbs) that are also being explored.

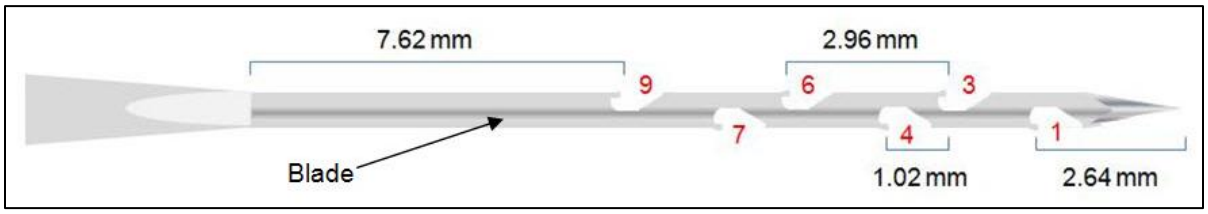

Figure 5. Illustration of the needle used in this investigation.

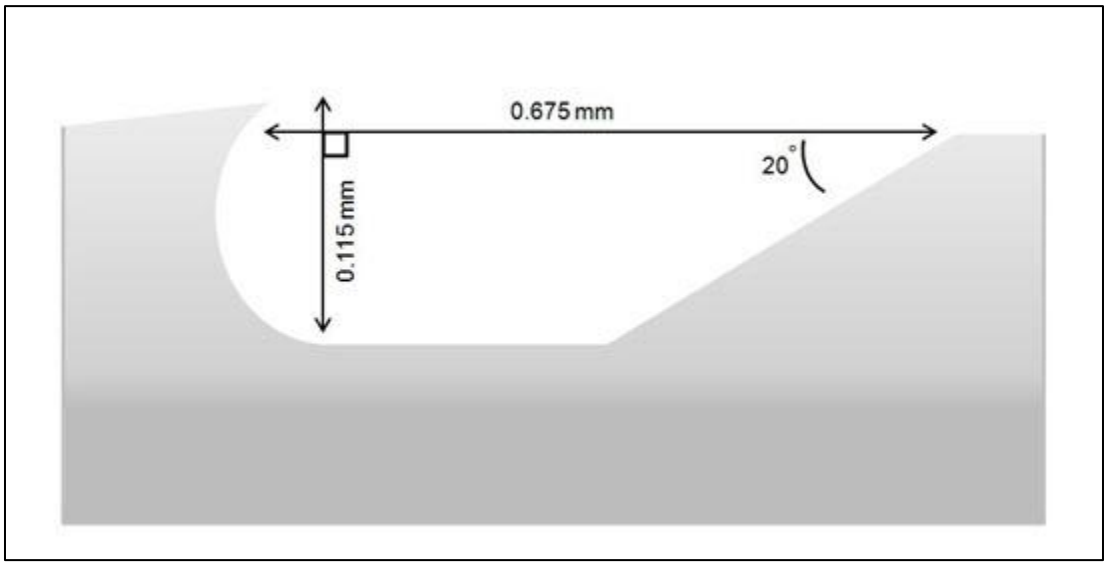

Figure 6. Detail of the barb for the needle used in this investigation.

3.3 Needling Processes

Needling of Panel 1 was performed entirely by hand used a commercial off the shelf (COTS) "felting" tool designed for wool arts/crafts projects (e.g., decorating articles of clothing) as shown in figure 7a. The detail in figure 7b shows five needles installed in the tool. Four needles were loaded into the felting tool in a spacing of approximately 13 mm (½ inch) square. In an attempt to process a uniformly reinforced plate, 13 mm-spaced gridlines were lightly drawn with a marker on the top layer of aramid with the purpose of guiding the needling operation to achieve

a uniform distribution of TTR. At each gridline crossing, the needles were plunged through the laminate and partially into a foam backer until the aramid was locally depleted at that point. This required approximately 20 plunges of the four-needles per grid crossing. The depth of each plunge was not controlled beyond ensuring that all nine barbs of each needle entered the laminate.

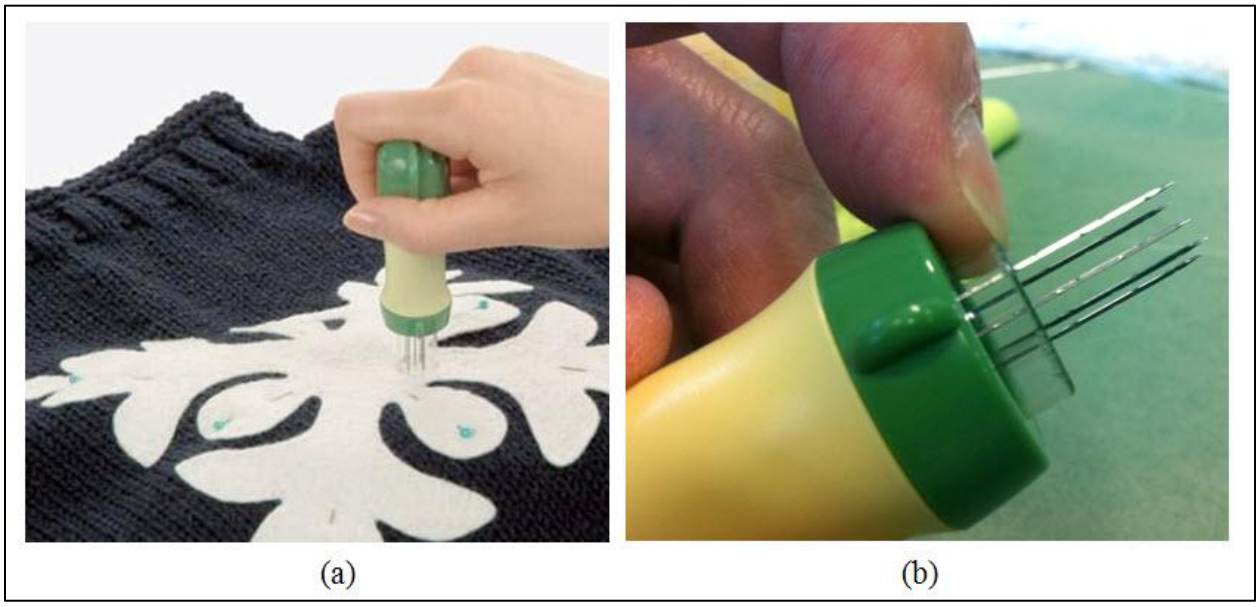

Figure 7. (a) Photo of felting tool in-use for a clothing art/craft (*8*); (b) detail of needles in the tool at the ARL composites laboratory.

At the conclusion the needling process, the preform was removed from the foam backer that was removed before the panel was processed with VARTM. A significant quantity of aramid could be seen protruding from the backside of the laminate as well as embedded in the foam backer, indicating inefficiency in this handheld processing method. After the panel was processed with VARTM, the TTR was observed in localized "clumps" on the bottom of the panel (presumably at the gridline crossings), and the panel exhibited thickness variations between 5.8 and 7.8 mm in the processed area.

Needling of Panel 2 was performed with semi-automated fixturing in an attempt to address the major deficiencies of the handheld process used in Panel 1, namely depth control, and spatial uniformity in the penetrations. Two plies of the aramid mat were placed on top and bottom of the laminate as shown in figure 5. A variable-speed jigsaw was modified with an array of needles (in place of the standard blade) and an adjustable height shoe that served to set the needle stroke such that needles' barb #1 just barely penetrated the bottom of the laminate. The jigsaw is shown in figures 8a and 8b shows a detail of the four-needle fixture and the adjustable-height shoe. The forward speed of the jigsaw was controlled by hand. A length of bar stock was used as a fence to guide the jigsaw during processing and was carefully indexed sideways after each pass of the jigsaw. The photograph in figure 8c shows the uniformity of the plunges, each

plunge spaced approximately 3 mm from neighboring holes. Two perpendicular sets of passes were made on the top side, then the preform was flipped over and two perpendicular passes were made on the other side.

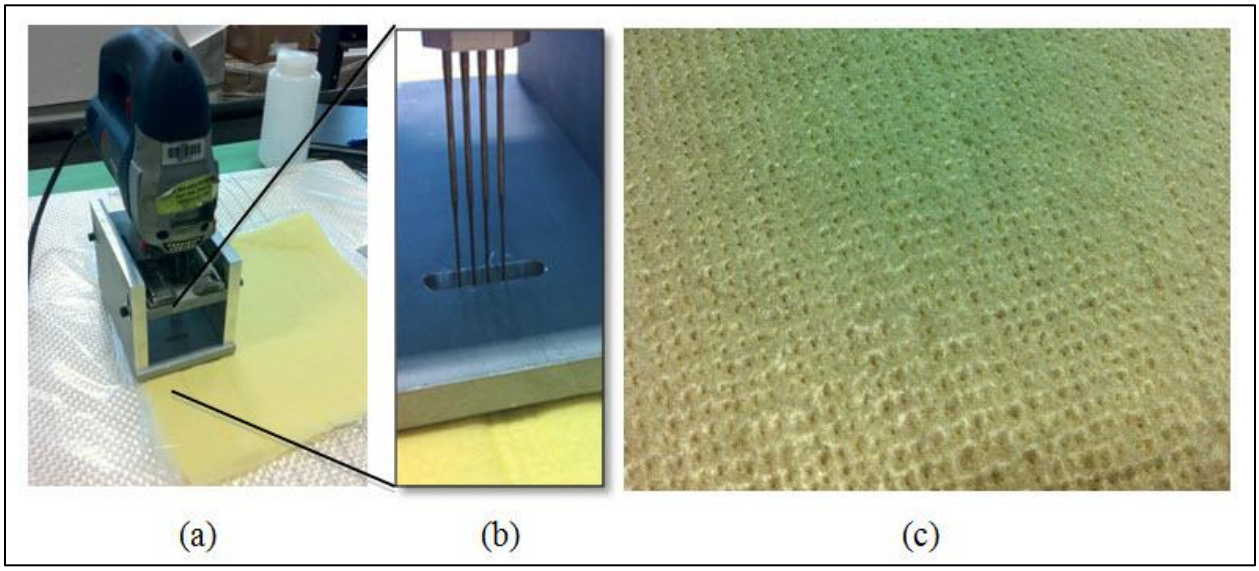

Figure 8. (a) Jigsaw ready for needling; (b) detail showing needle array and adjustable-height shoe; and (c) resultant uniformly-spaced penetration holes visible in the aramid mat.

Instead of using a foam backer, this laminate was supported with an aluminum plate covered with six plies of woven glass and a sheet of polyethylene. This support arrangement retains sufficient permeability for the needles and deflects much less than the foam backer. This change was made to facilitate control of the penetration depth of the needles during processing.

Attempts were made to peel off the semi-depleted aramid layers after needling in order to produce monolithic samples to more easily compare the needled and non-needled materials. These attempts resulted in seemingly large amounts of pullout of the TTR from the laminate. As such, the authors decided to leave the post-needled aramid layers in place and part of the final VARTM structure.

3.4 Experiments and Samples

Low velocity impact (LVI) testing was carried out according to ASTM D7136 (*9*) with the exception of the energy level (drop mass × height). The standard method calls for an energy level that induces "barely visible" impact damage by impacting the samples at 6.7 J per mm of sample thickness. For the samples under investigation here that standard energy level would be approximately 36 J. We used impact energy of 100 J to impart more than "barely visible" damage to the materials. All samples were impacted on the smooth tool-side.

Compression after impact (CAI) testing was conducted according to ASTM D7137 (*10*). All samples failed with the acceptable "LDM" failure mode wherein the "L" means lateral, the "D" means at/through damage, and the "M" means middle of the sample. Samples were not instrumented with strain gages.

To assess the effects of needling on undamaged material, compression tests were performed according to ASTM D6641M (*11*), and four-point bend testing was carried out using ASTM D6272 (*12*). Samples were not instrumented with strain gages.

Table 1 lists the areal densities and dimensions of the samples for the various mechanical tests performed on the two panels. Baseline samples that did not incorporate aramid and were not needled were processed separately from the needled/control panels. Needling was found to thicken the materials by 2.6% to 3%, resulting in slightly higher areal densities compared to the control samples. Fiber volume fractions of TTR were not measured for either panel but are estimated to be in the range of 1 to 2%.

Several cubes of material were cut from Panel 1 then mounted and polished to microscopically observe the quality of the needled TTR. Optical micrographs of material cross-sections are presented in the section 4.

The authors considered testing samples that were needled in the absence of aramid mat to assess effects of any damage caused by needling (e.g., fiber breakage in the laminate). Proper fabrication of such a sample is, however, complicated because during the normal needling process the barb is filled with mat and thus the downward-facing barb (the damaging part of the needle) never fully engages the in-plane fibers. As such, no attempt was made to assess the effects of the needles alone.

Table 1. Sample areal densities and dimensions for the various tests performed on the panels in this investigation.

	Areal Density Kg/m^2 (psf)	**LVI and CAI mm**	**Compression mm**	**4-pt bend mm**
		length × width × thickness		
Baseline	9.369±0.02 (1.92±0.00)	152 × 102 × 5.40±0.07	NA	NA
Panel 1 control	9.92±0.06 (2.03±0.01)	152 × 102 × 6.31±0.11	NA	NA
Panel 1 needled	10.68±0.28 (2.19±0.06)	152 × 102 × 6.50±0.55	NA	NA
Panel 2 control	10.74±0.04 (2.20±0.01)	152 × 102 × 6.67±0.09	13 × 140 × 6.67±0.09	13 × 102 × 6.67±0.09
Panel 2 needled	11.01±0.03 (2.25±0.01)	152 × 102 × 6.85±0.16	13 × 140 × 6.85±0.16	13 × 102 × 6.85±0.16

4. Results/Discussion

4.1 LVI

Figure 9 shows the data collected during LVI testing of baseline samples and Panel 1 needled and control samples. The average response of three samples for each test condition is shown. Needled samples exhibited slightly higher peak impact force (figure 9a) and significantly less deflection (figure 9b), resulting in a material that is effectively stiffer under impact conditions. Figure 9c is a plot of the force-displacement response (effective stiffness) for the three materials, showing that the needled samples are 10–15% stiffer than the control samples. A portion of this apparent improvement in stiffness is due to the 3.0% increase in material thickness resulting from the needling process, but a portion is due to shifting the failure mode from delamination to through-thickness shear failure. The energy absorption behavior (figure 9d) shows that all sample types absorb 60 J. It is interesting to note that the baseline and control samples exhibit almost identical response for these four metrics, indicating that the aramid has negligible influence on the mechanical response of the material under impact loads. Again, all samples were impacted tool-side-up (aramid-side-down).

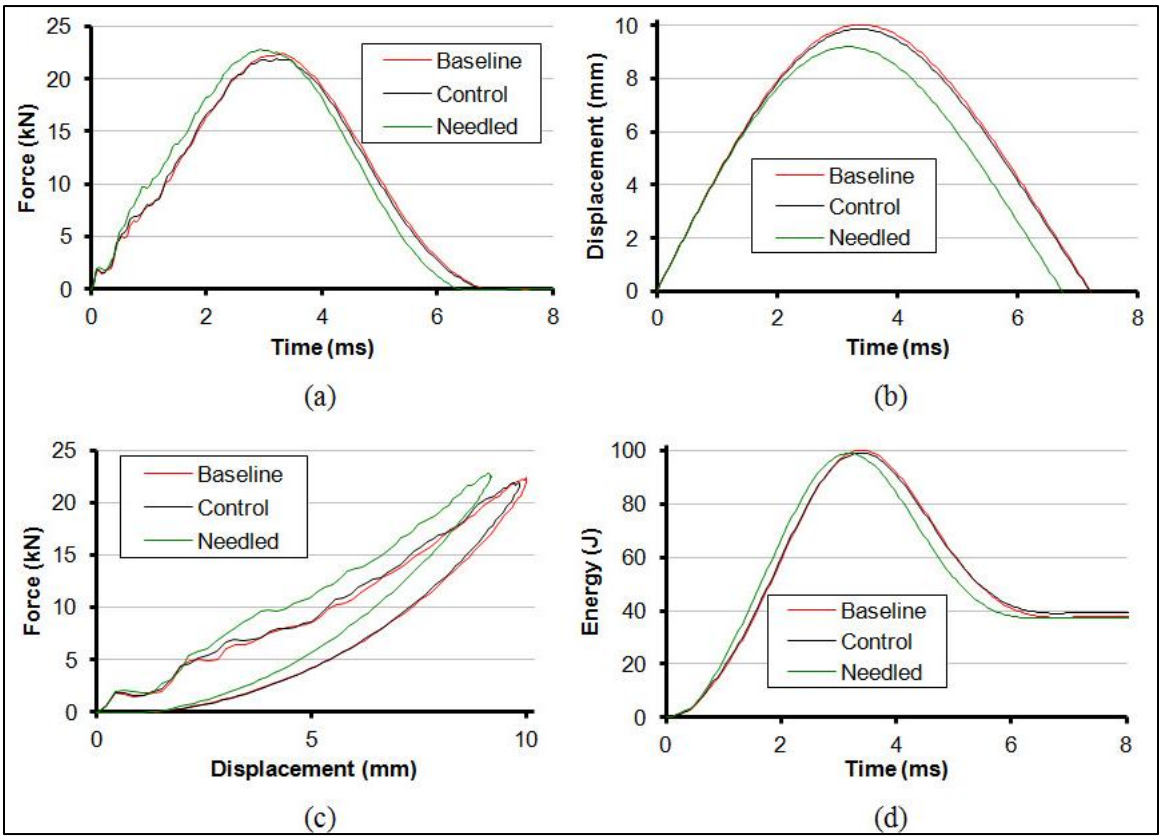

Figure 9. (a) Force vs Time; (b) Displacement vs Time; (c) Force vs. Displacement; and (d) Energy vs. Time for the samples from Panel 1.

Figure 10 shows the data collected during LVI testing of baseline samples and Panel 2 needled and control samples. The control samples from this panel do markedly differ in response from the baseline samples (same baseline data from figure 9), exhibiting significantly higher stiffness. Part of this difference may be attributed to the fact that these control samples had aramid on the top and bottom of the sample. This will slightly increase the bending stiffness of the sample but more importantly will reduce and/or delay crushing damage on the laminate surface caused by the impactor. Similar to the results from Plate 1, needling increased the material thickness by 2.7% and the effective stiffness of samples from Plate 2 by 10–15% (figure 9c). Also like Panel 1, needled and control samples from Panel 2 ultimately absorbed approximately 60 J of the impact energy.

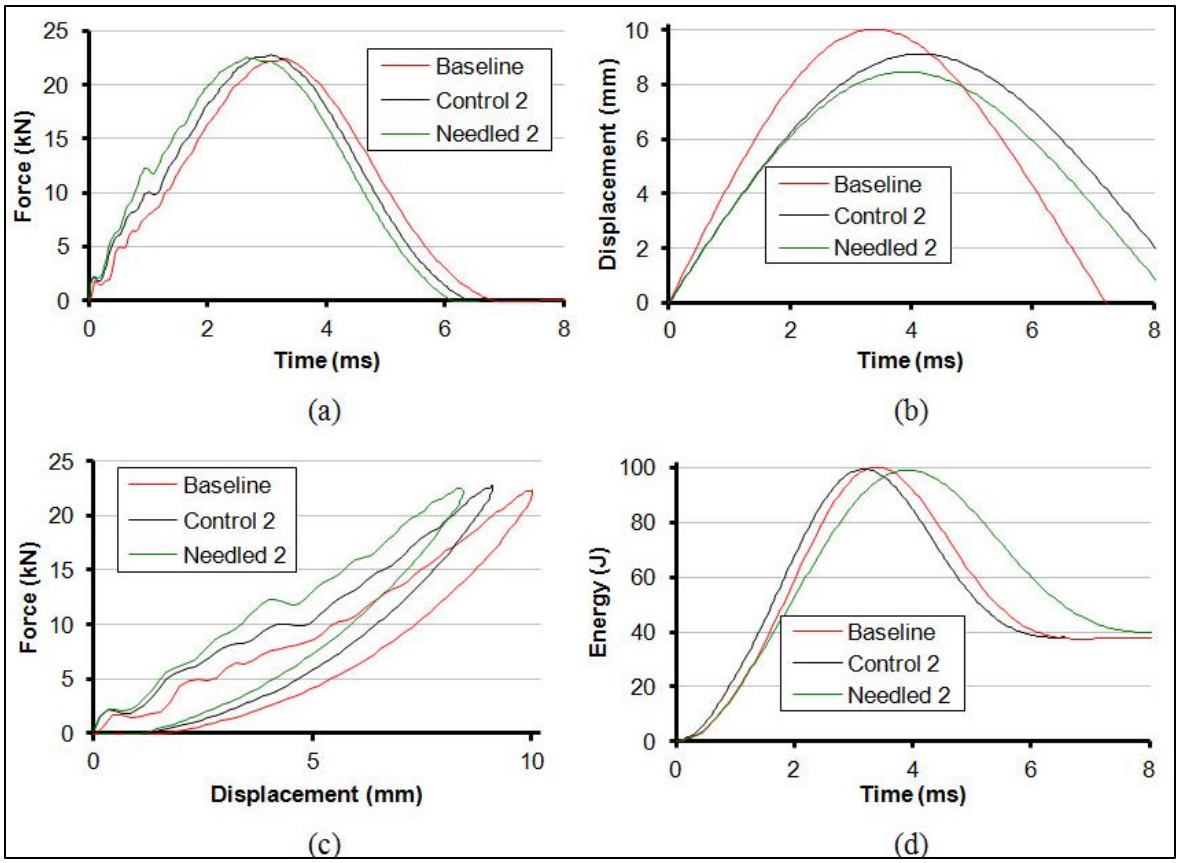

Figure 10. (a) Force vs Time; (b) Displacement vs Time; (c) Force vs. Displacement; and (d) Energy vs. Time for the samples from Panel 1.

4.2 Delamination Area

All specimens were digitally photographed on a lightbox to assess the delamination areas resulting from the impact testing. The brightness and contrast of the images were adjusted by-eye to more clearly distinguish the delamination boundaries. The software package "ImageJ" (*13*) was used to trace the boundaries (again, by eye) and quantify the delamination area. Figures 11a–e show the images for all impact samples reported in the results above, and figure 12 summarizes the delamination areas in a column plot. The inclusion of aramid in the control samples reduced the delamination areas by 4% to 8% relative to the baseline samples. Needled samples from Panel 1 exhibited 59% less delamination area relative to Control samples from panel 1 and likewise Needled samples from Panel 2 exhibited 36% less delamination area.

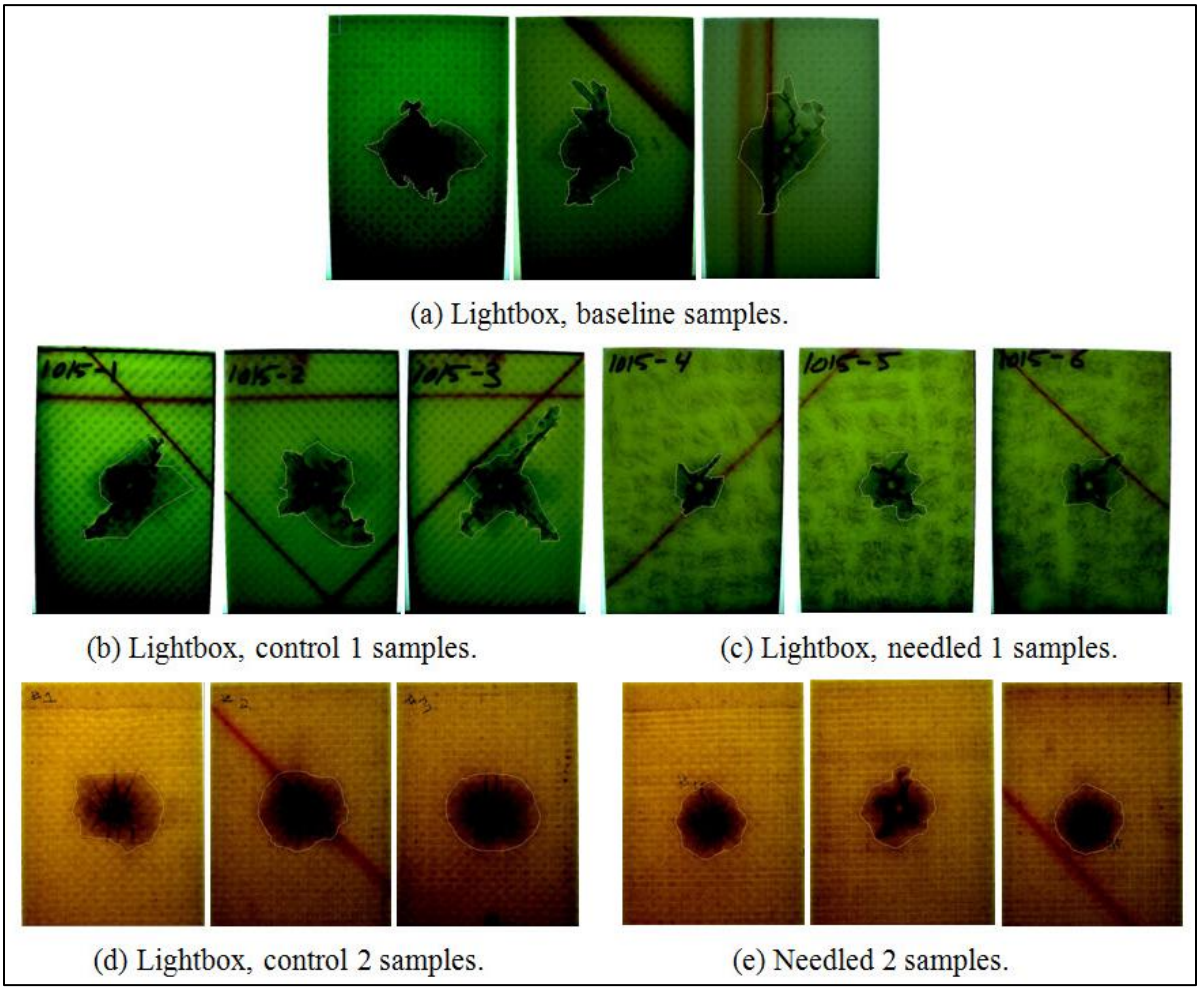

Figure 11. (a) Lightbox, baseline samples; (b) lightbox, control 1 samples; (c) lightbox, needled 1 samples; (d) lightbox, control 2 samples; and (e) needled 2 samples.

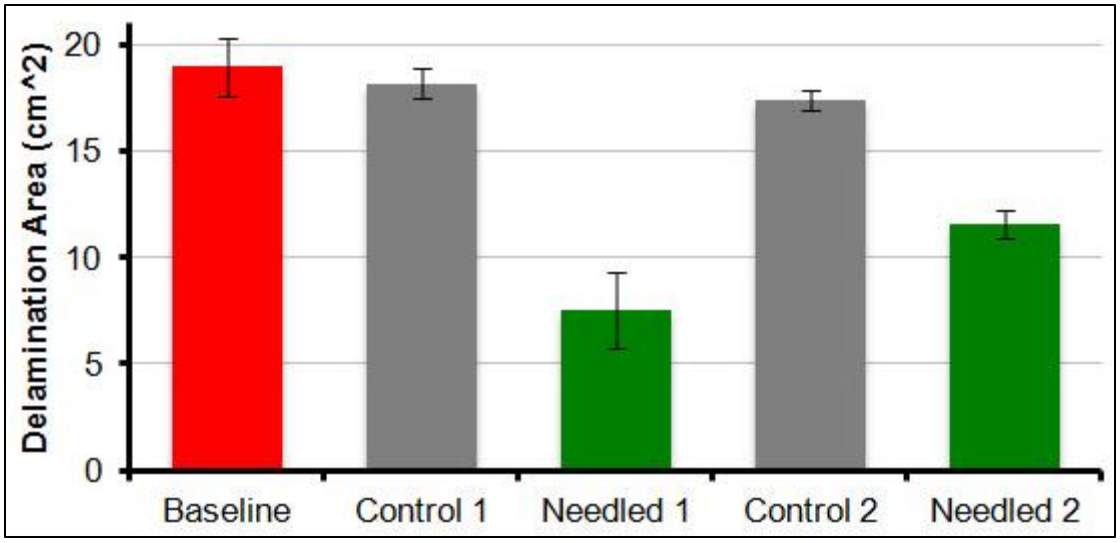

Figure 12. Comparison of delamination areas for all impacted samples.

4.3 Compression After Impact (CAI)

Figures 13 and 14 show the results of CAI testing for the impacted samples. Stresses for all samples were calculated based on the cross-sectional area of the baseline samples in order to most-fairly compare the structural response of the laminates, which all had the same amount of in-plane reinforcement. Compared to the control samples, the compression-after-impact strength of the needled materials improved by 30% to 40%, reflecting the fact that needled samples sustained smaller delamination areas from the impacts.

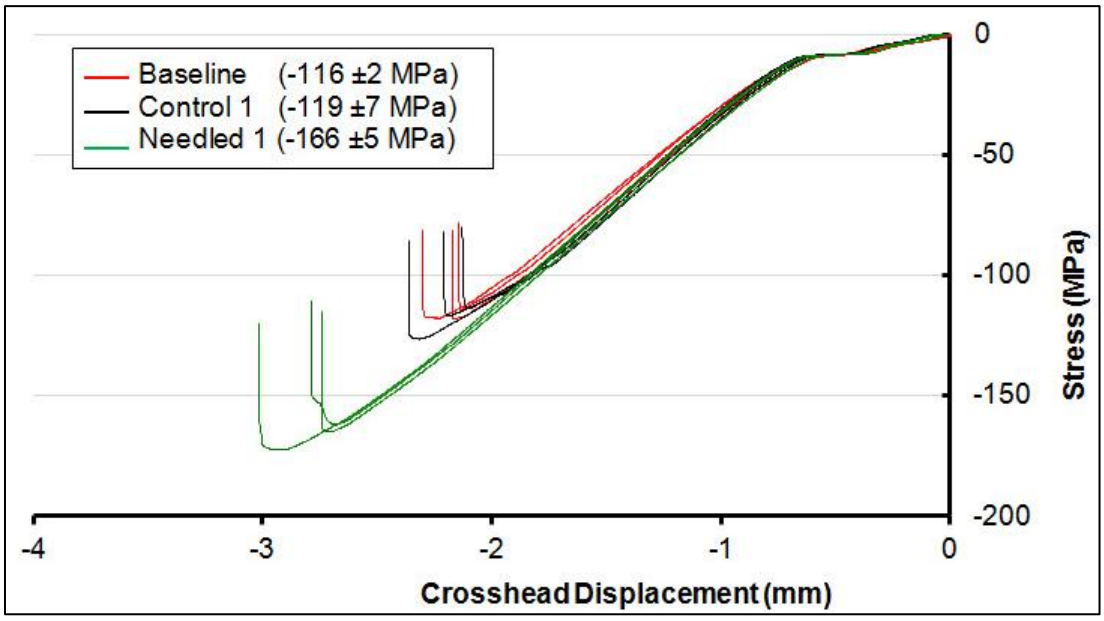

Figure 13. Compression after impact for Baseline and Panel 1 samples.

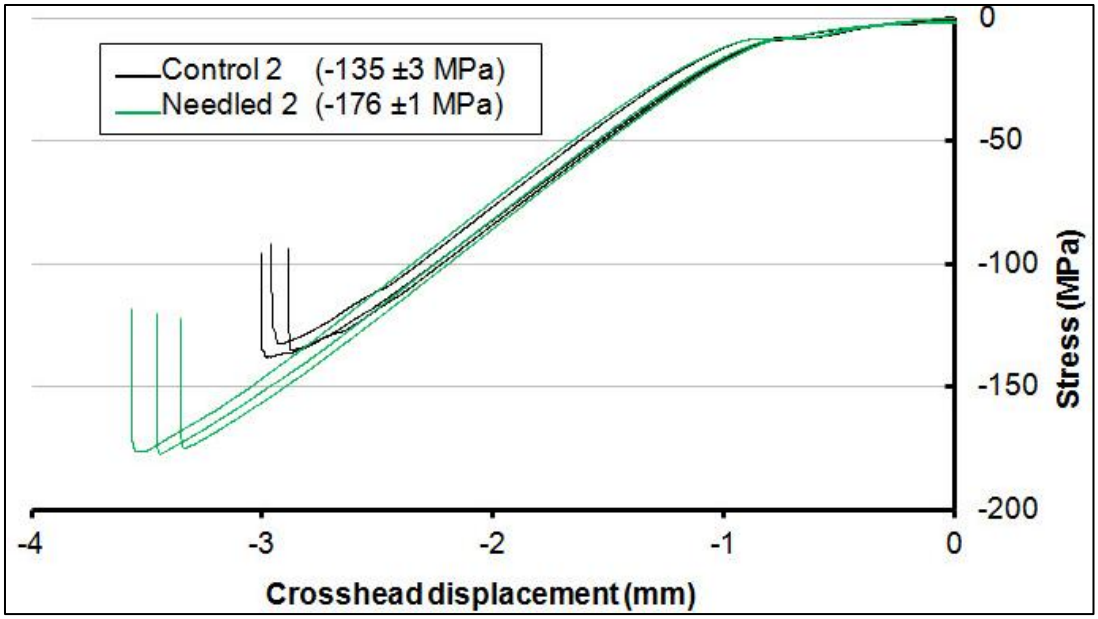

Figure 14. Compression after impact for Panel 2 samples.

4.4 Compression and Flexural Strength

Figure 15 shows the results of compressive testing for samples cut from un-impacted portions of Panel 2. Samples from Panel 1 were not tested in kind due to poor geometric uniformity of the needled material. Like the CAI results, in order to most fairly compare the results of the control and needled specimens, the stress for all compression samples was calculated based on the thickness of the Control samples. Although the needled samples were slightly thicker, both sample types contained equal amounts of in-plane reinforcement. A 9% increase in compressive strength of needled specimens is observed and likely indicates that the TTR is stabilizing the buckling instability of the laminate.

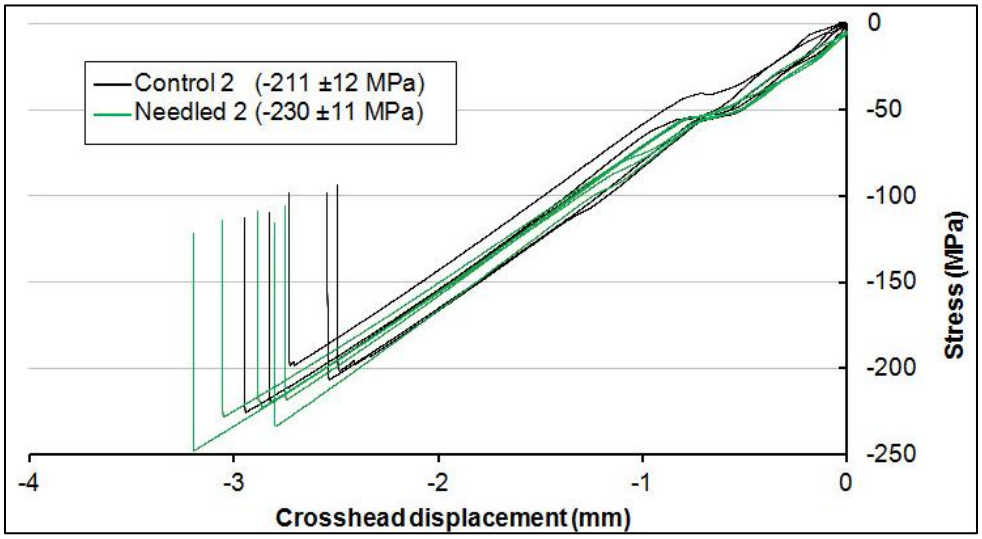

Figure 15. Compression strength results for Panel 2.

Figure 16 shows the results of flexural testing of samples cut from un-impacted portions of Panel 2. Samples from Panel 1 were not tested in kind due to poor geometric uniformity of the needled material. The actual thickness and width dimensions of each sample were used to calculate the "Maximum Fiber" stresses and strains in figure 16, using the mechanics-of-materials equations 6 and 10 from the ASTM (*10*). Needled samples exhibited a 17% improvement in ultimate flexural strength compared to control samples. The formation and growth of delamination cracks was not tracked visually during testing. Such observations may have provided insight on the physical mechanism causing the TTR material to exhibit higher flexural strength. Figure 16 shows that the flexural load of the needled material increased monotonically to very near peak for all samples, whereas the load history of the control material exhibited several small non-monotonic drops (which were audible) well prior to peak.

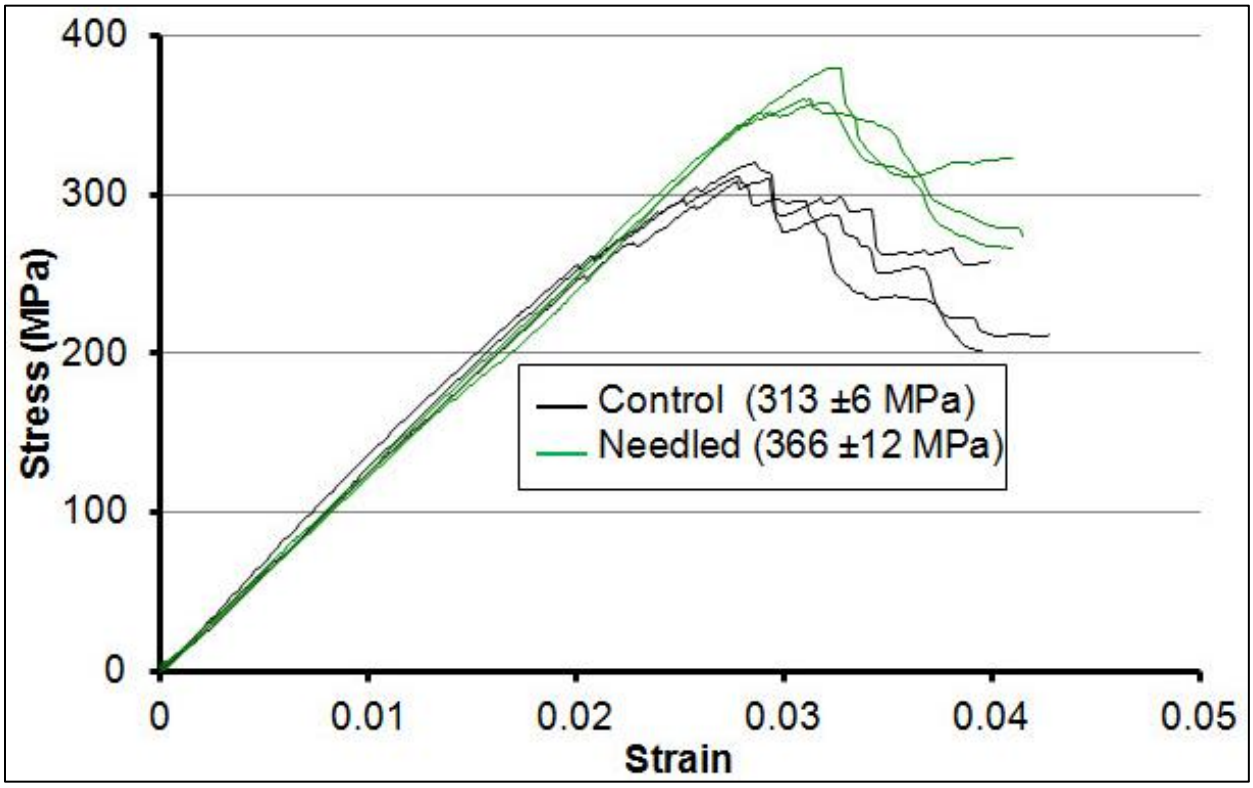

Figure 16. Flexural strength results for Panel 2.

4.5 Microstructure

The micrograph in figure 17 shows one of the better cross-sections observed in the microscopy samples. This image reveals the relative sparsity and "meandering" nature of the TTR. The blurry-looking TTR filaments appear so because they are not on the polished surface, rather they are located within the volume of the sample. The meandering bundles are more closely shown in figure 18 and reflect the lack of control (fixity) over the laminate while processing Panel 1. Such images served as the impetus to change the process for Panel 2 – most importantly increasing the stiffness of the backer (as shown in figure 5) and using a semi-automated tool for needling instead of a hand-held tool. Similar micrographs from Panel 2 were not captured.

It is interesting to observe in the micrographs that the TTR bundles are comprised of a small number of filaments (say, several dozen in each bundle). This morphology is a key feature distinguishing needled reinforcement from those achievable with the tufting and stitching processes (thousands of filaments in those TTR threads).

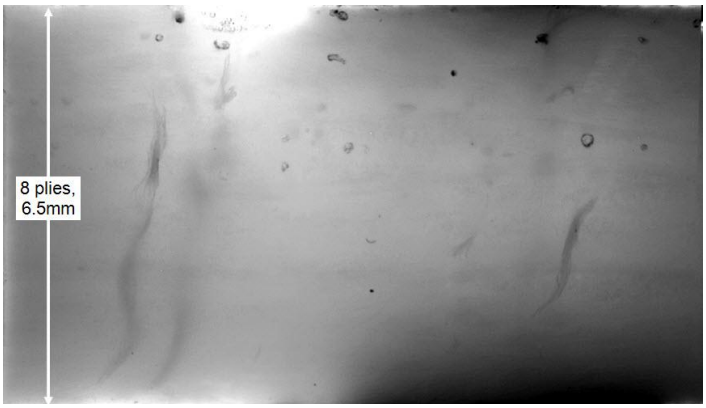

Figure 17. Through-thickness cross-section showing several filament bundles of aramid in the through-thickness direction.

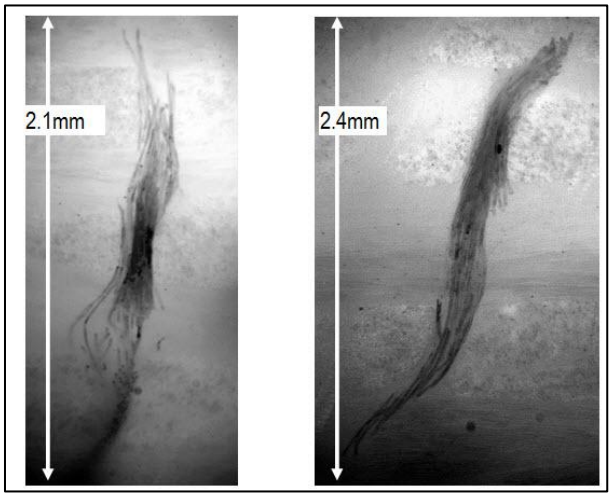

Figure 18. Details from the micrograph shown in figure 16.

5. Conclusions and Continuing/Future Work

Knowledge has been gained with the processing of needled composites. Despite the fact that the needles and aramid mat materials acquired for this investigation were not designed for the purpose of creating 3D-reinforced structural composites, we were able to use them to process two 3D-reinforced "proof of concept" needled-TTR panels. These panels exhibited significantly improved impact resistance without the reductions in stiffness and strength that are observed with tufted and stitched materials.

The original intent of this work was to begin investigation into the microstructure of needled composite material to guide the eventual development of a process model. Micrographs of sectioned samples indicate that effort should first be invested in mechanizing the needling process, which is currently underway. When complete, the mechanized process will enable parametric control of the TTR in processed panels and it should result in better morphological quality (e.g., straightness) of the bundles.

The plan is to fabricate thicker panels and panels with angled reinforcements to further improve bending stiffness and mode II fracture toughness. After the processing equipment is in-place and being used to process these novel materials, the resultant microstructure will be evaluated using micro-CT and used to create a representative volume element for finite element analysis.

6. References

1. Mouritz, A. P.; Leong, K. H.; Herszberg, I. A Review of the Effect of Stitching on the In-plane Mechanical Properties of Fibre-reinforced Polymer Composites. *Composites: Part A* **1997**, *28A*.
2. Cartie, D. et al. 3D Reinforcement of Stiffener-to-skin T-joints by Z-pinning and Tufting. *Engineering Fracture Mechanics* **2006**, *73*.
3. Dell'Anno, G. et al. Exploring Mechanical Property Balance in Tufted Carbon Fabric/Epoxy Composites. *Composites: Part A* **2007**, *38*.
4. Colin de Verdiere, M. Evaluation of the Mechanical and Damage Behaviour of Tufted Non Crimped Fabric Composites Using Full Field Measurements. *Composites Science and Technology* **2009**, *69*.
5. Potluri, P. et al. Bench-Marking Of 3D Preforming Strategies. *ICCM 17 Proceedings*, 2009. 27-31 July 2009, Edinburgh, UK.
6. Pierson, H. O.; Northrop, D. A. Carbon-Felt, Carbon-Matrix Composites: Dependence of Thermal and Mechanical Properties on Fiber Precursor and Matrix Structure. *Journal of Composite Materials* **1975**, *9* (118).
7. Han, C-L. et al. Microstructure and Mechanical Property of Three-Dimensional Needled C/SiC Composites Prepared by Precursor Pyrolysis. *Key Engineering Materials* **2010**, *434–435*.
8. http://thesilverpenny.homestead.com/KitsNeedlefelting.html (accessed 2012).
9. ASTM D7136M-05, 2005, Standard Test Method for Measuring the Damage Resistance of a Fiber-Reinforced Polymer Matrix Composite to a Drop-Weight Impact Event, ASTM International, West Conshohocken, PA.
10. ASTM D7137M-05, 2005, Standard Test Method for Compressive Residual Strength Properties of Damaged Polymer Matrix Composite Plates, ASTM International, West Conshohocken, PA.
11. ASTM D6641M-01, 2001, Standard Test Method for Compressive Properties of Polymer Matrix Composite Materials Using End Loaded Side Support Test Fixture, ASTM International, West Conshohocken, PA.
12. ASTM D6272-02, 2002, Standard Test Method for Flexural Properties of Unreinforced and Reinforced Plastics and Electrical Insulating Materials by Four-Point Bending, ASTM International, West Conshohocken, PA.
13. ImageJ software, http://rsbweb.nih.gov/ij/ (accessed 2012).

NO. OF COPIES	ORGANIZATION
1 ELEC	ADMNSTR DEFNS TECHL INFO CTR ATTN DTIC OCP 8725 JOHN J KINGMAN RD STE 0944 FT BELVOIR VA 22060-6218
1	US ARMY INFO SYS ENGRG CMND ATTN AMSEL IE TD A RIVERA FT HUACHUCA AZ 85613-5300
15	US ARMY RSRCH LAB ATTN RDRL WMM A R EMERSON ABERDEEN PROVING GROUND MD 21005
3	US ARMY RSRCH LAB ATTN IMAL HRA MAIL & RECORDS MGMT ATTN RDRL CIO LL TECHL LIB ATTN RDRL CIO LT TECHL PUB ADELPHI MD 20783-1197

TOTAL: 20 (1 PDF, 19 HCS)